

# Néel transition and $\gamma \rightleftharpoons \varepsilon$ transformation in polycrystalline Fe–Mn–Si shape memory alloys

QIN ZUOXIANG, YU MANPING\*, ZHANG YANSHENG

*Department of Materials Science and Engineering, Dalian Railway Institute, Dalian 116028, People's Republic of China*

Silicon lowers the Néel temperature,  $T_N$ , and enhances the paramagnetic characteristic of  $\gamma$ -Fe–Mn alloy, which results in a reduction of the stability of austenite and in the anomalous increase of electrical resistivity,  $\rho$ , below  $T_N$  becoming stronger, i.e. the anomalous  $\rho$  below  $T_N$  increases rapidly with increasing silicon content. The  $\gamma \rightleftharpoons \varepsilon$  transformation occurs during cooling and heating, but  $\gamma \rightarrow \varepsilon$  martensitic transformation is suppressed below about 240 K, probably due to the  $\varepsilon$  phase transfer from paramagnetic to antiferromagnetic state. The  $\rho(T)$  changes steeply, accompanying the Néel transition and the  $\gamma \rightleftharpoons \varepsilon$  transformation. Silicon increases the electrical resistivity and the magnetic susceptibility,  $\chi$ , of  $\gamma$ -Fe–Mn alloy, and the  $\varepsilon$  phase obviously increases the electrical resistivity of Fe–Mn–Si alloys. The relation between the Néel transition,  $\gamma \rightarrow \varepsilon$  martensitic transformation and shape memory effect (SME), are discussed.

## 1. Introduction

The Néel transition and the  $\gamma \rightarrow \varepsilon$  transformation are two typical physical phenomena of  $\gamma$ -Fe–Mn alloys. With increasing manganese content, the Néel temperature,  $T_N$ , rises and austenite form is stabilized against  $\gamma \rightarrow \varepsilon$  martensitic transformation during cooling [1, 2], so that the austenitic  $\gamma$ -Fe–30 Mn alloy is still stable at very low temperature. However, the  $\gamma \rightarrow \varepsilon$  martensitic transformation occurs with the addition of some silicon into  $\gamma$ -Fe–30 Mn alloy [3–6]; this is due to the addition of a small amount of silicon which reduces the Néel temperature and stacking fault energy (SFE). In recent years, Fe–Mn and Fe–Mn–Si alloys have gained much attention because of their complete shape memory effect (SME). The origin of SME of Fe–Mn–Si alloys arises from non-thermoelastic stress-induced  $\gamma \rightarrow \varepsilon$  martensitic transformation and its  $\varepsilon \rightarrow \gamma$  reverse transformation, which is distinct from the thermoelastic martensite transformation origin of Ni–Ti and Cu–Zn–X [3–5]. Many researchers have reported that the SME is sensitive to the composition [2, 6, 7], physical properties [5] and training [8]. Therefore, it is very important to understand the behaviour of the Néel transition and  $\gamma \rightleftharpoons \varepsilon$  transformation of Fe–Mn–Si alloys. In this work, the Néel transition and the  $\gamma \rightleftharpoons \varepsilon$  transformation in polycrystalline Fe–Mn–Si shape memory alloys have been studied by measuring the magnetic susceptibility and electrical resistivity corresponding to temperature.

## 2. Experimental procedure

Alloys were prepared by induction furnace melting under an argon atmosphere of about 760 mm Hg, using low-carbon iron, electrolytic manganese, pure silicon and chromium. The chemical compositions of the alloys are listed in Table I. Ingots were forged into bars (18 mm  $\times$  18 mm) and then heated at 1273 K for 1 h. Specimens were sealed in quartz tubes and again annealed at 1273 K for 1 h, and subsequently air-cooled.

Specimens for optical metallography were etched in a solution of 13% Nital–alcohol after electrolytic polishing. The magnetic susceptibility versus temperature curve ( $\chi$ - $T$  curve) was measured with a type MB-2 magnetic balance from 80–600 K. The electrical resistivity versus temperature curve ( $\rho$ - $T$  curve) was measured by the standard four-lead technique in which the voltage drops were obtained by a precision voltmeter with a resolution of  $1.0 \times 10^{-8}$  V. The Néel temperature was determined by a magnetic method and the onset temperature of the  $\gamma \rightarrow \varepsilon$  forward transformation,  $M_s$ , and the start and finishing temperature of the  $\varepsilon \rightarrow \gamma$  reverse transformation,  $A_s$  and  $A_f$ , were measured by the electrical resistivity method. The SME was measured by bend tests according to Sato *et al.* [3], using rectangular specimens 90 mm  $\times$  3.0 mm  $\times$  1.0 mm.

## 3. Results and discussion

### 3.1. Optical microstructure observation

The optical microstructures of alloys tested at room temperature are shown in Fig. 1. Many  $\varepsilon$  martensite

\* Present address: Dalian Acid-proof Pump Plant, Dalian 116022, People's Republic of China.

TABLE I Chemical compositions, phase transformation temperatures, and shape memory effect of the experimental alloys

Code	C (wt %)	Mn (wt %)	Si (wt %)	Cr (wt %)	$M_s$ (K)	$A_s$ (K)	$A_f$ (K)	$T_N$ (K)	SME (%)
1	0.016	27.77	4.10	–	352	425	450	300	35
2	0.017	31.81	5.22	–	320	390	412	290	78
3	0.017	32.01	6.10	–	300	390	415	277	82
4	0.021	31.59	6.19	2.06	290	390	415	278	82

plates are formed in Fe–27.7 Mn–4.1 Si alloy when the specimen cools from 1273 K to room temperature, in which the phenomenon of intersections between the  $\epsilon$  martensitic plates is observed (Fig. 1a). There is a little  $\epsilon$  martensite in Fe–31.8 Mn–5.2 Si alloy (Fig. 1b) and very little  $\epsilon$  martensite in Fe–32.0 Mn–6.1 Si and Fe–31.6 Mn–6.2 Si–2 Cr alloys (Fig. 1c and d). The results agree with those of X-ray diffraction.

### 3.2. Néel transition and $\gamma \rightleftharpoons \epsilon$ transformation

The magnetic susceptibility,  $\chi$ , versus temperature curves of Fe–27.7 Mn–4.1 Si, Fe–31.8 Mn–5.2 Si and Fe–32.0 Mn–6.1 Si alloys during heating from 80–600 K are shown in Fig. 2. The phase transformation temperatures, marked by arrows,  $T_N$ ,  $A_s$  and  $A_f$ . Silicon increases  $\chi$  and reduces  $T_N$ , the peak at the Néel point becoming higher and sharper with increas-

ing silicon content. Below  $T_N$ , the  $\gamma$  phase of the alloys is in the antiferromagnetic state, and  $\chi$  increases with increasing temperature. Above  $T_N$ , the  $\gamma$  phase is in the paramagnetic state,  $d\chi/dT$  is negative, and  $\chi$  decreases with increasing temperature. The temperature dependence of  $\chi$  obeys the Curie–Weiss law, which indicates that silicon enhances the paramagnetic characteristic. The magnetic behaviour of Fe–Mn–Si shape memory alloys is similar to that of Fe–Mn–Al–C and Fe–Mn–Si–C alloys [9–16], suggesting the existence of a localized moment in Fe–Mn alloys by adding elemental silicon, which is supported by the linear dependence of internal magnetic fields on the silicon content [17]. The  $T_N^{\epsilon}$  is not determined, but according to Ohno and Mekata [18], the  $T_N^{\epsilon}$  which is almost composition independent is about 230 K.  $\chi$  increases when  $\epsilon \rightarrow \gamma$  reverse transformation occurs.

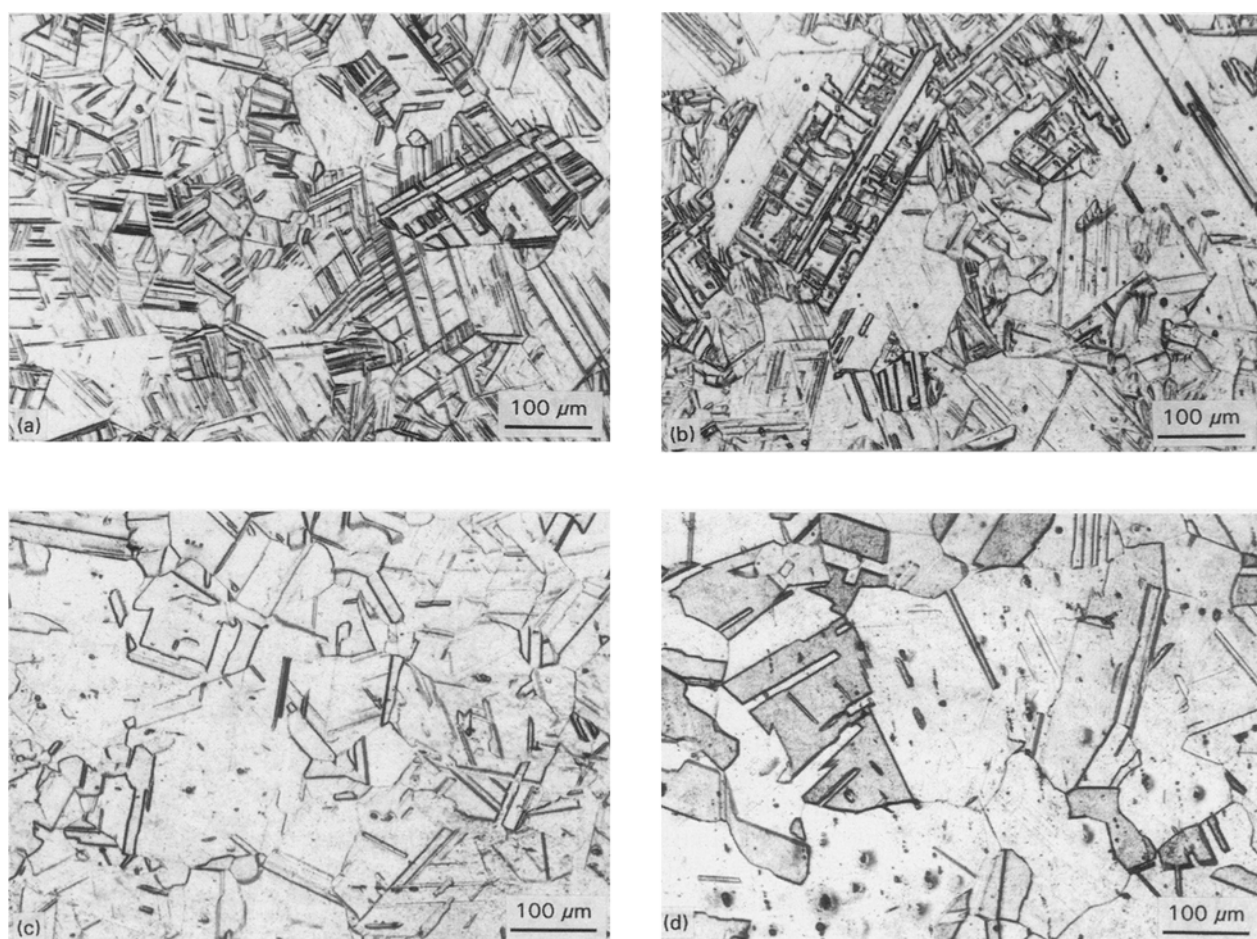


Figure 1 Optical microstructure for Fe–Mn–Si alloys at room temperature: (a) Fe–27.7 Mn–4.1 Si, (b) Fe–31.8 Mn–5.2 Si, (c) Fe–32.0 Mn–6.1 Si, (d) Fe–31.6 Mn–6.2 Si–2 Cr.

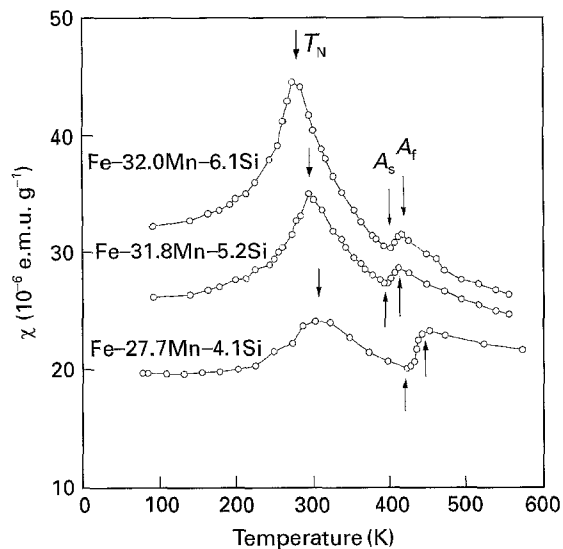


Figure 2 The magnetic susceptibility versus temperature curves of Fe-Mn-Si alloys.

As shown in Fig. 3, the Néel transition and  $\gamma \rightleftharpoons \epsilon$  transformation have strong effects on the electrical resistivity,  $\rho$ , versus temperature curves of alloys. The phase transformation temperature determined by the electrical method are listed in Table I, which are in agreement with those obtained by the magnetic method. It is found that the amount of  $\epsilon$  martensite is associated with  $M_S$  and  $(M_S - T_N)$ . Because the  $M_S$  of alloy Fe-27.7 Mn-4.1 Si is above room temperature, and  $M_S$  is much higher than  $T_N$ , large amounts of  $\epsilon$  martensite are found in alloy Fe-27.7 Mn-4.1 Si at room temperature. However, there is little  $\epsilon$  martensite in alloy Fe-31.8 Mn-5.2 Si and very little  $\epsilon$  martensite in Fe-31.6 Mn-6.2 Si-2 Cr and Fe-32.0 Mn-6.1 Si because the  $M_S$  of the alloys falls to almost room temperature and  $(M_S - T_N)$  is smaller. The  $\gamma \rightarrow \epsilon$  transformation is suppressed when the alloys transfer from the paramagnetic to antiferromagnetic state.

The electrical resistivity of alloys decreases linearly when specimens cool from 500 K because of phonon scattering. However, the  $\rho-T$  curves deviate from linearity at lower temperature. It was found that  $\rho$  is almost temperature independent in the range of 350 K

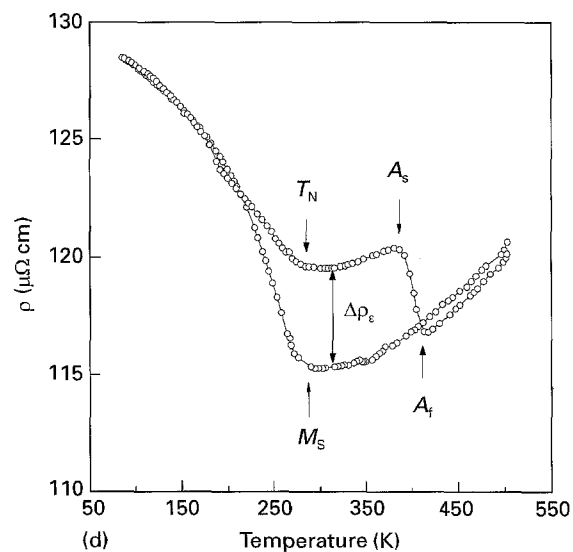
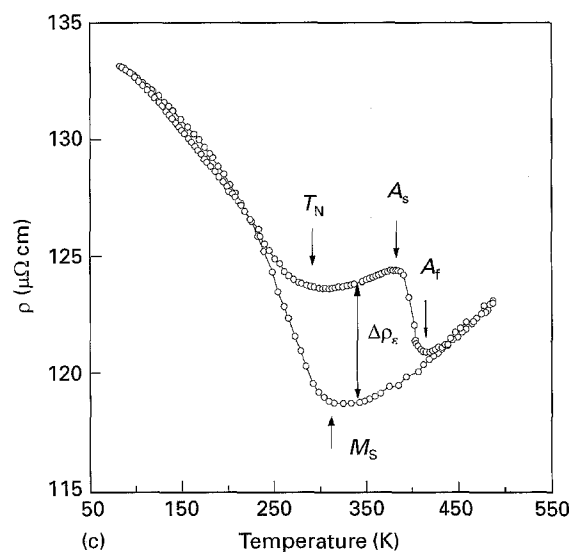
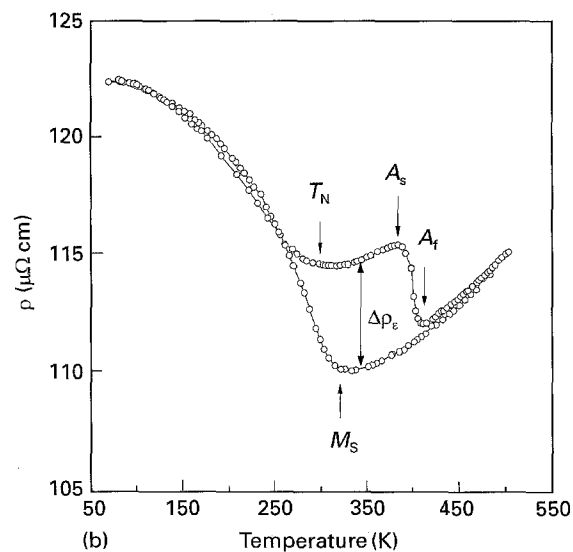
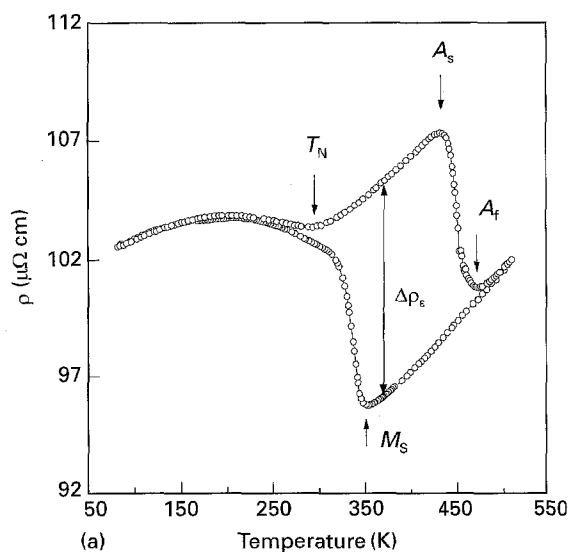


Figure 3 The electrical resistivity versus temperature curves of Fe-Mn-Si alloys. (a) Fe-27.7Mn-4.1 Si; (b) Fe-31.8 Mn-5.2 Si; (c) Fe-32.0 Mn-6.1 Si; (d) Fe-31.6 Mn-6.2 Si-2Cr.

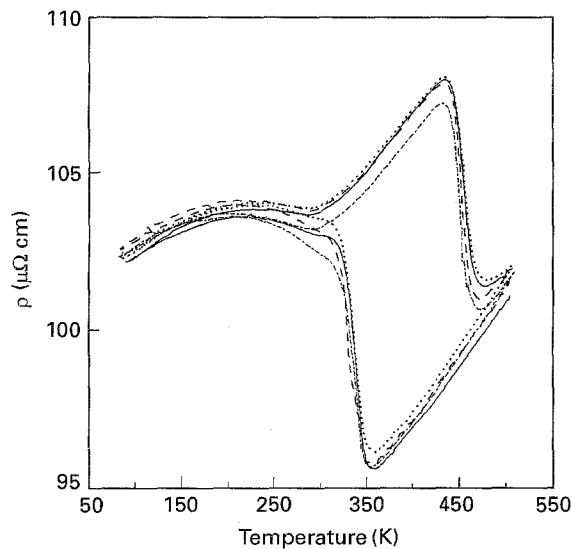


Figure 4 Effect of thermal cycling on the  $\gamma \rightleftharpoons \epsilon$  transformation: cycle (· - ·) 1, (---) 2, (—) 3, (···) 4.

to  $M_S$  for all the alloys except Fe-27.7 Mn-4.1 Si, which indicates that some changes occur in the alloys. The anomalous  $\rho$  increases abruptly during cooling to 80 K, which is attributed to slight  $\gamma \rightarrow \epsilon$  martensitic transformation and Néel transition. The derivative of the resistivity with respect to temperature,  $d\rho/dT$ , is negative, and the anomalous  $\rho$  increases with silicon content. When the temperature rises from 80 K, the  $\rho$ - $T$  cooling and heating curves overlap below about 240 K; this means there is no  $\epsilon$  martensite formed, and the  $\gamma \rightarrow \epsilon$  martensitic transformation is suppressed when the  $\epsilon$  phase is in the antiferromagnetic state, in which  $T_N^\epsilon$  is at about 230 K [18]. Because the  $\gamma \rightarrow \epsilon$  martensitic transformation increases  $\rho$  and the  $\epsilon \rightarrow \gamma$  reverse transformation reduces  $\rho$ , a quadrangle is formed by the  $\rho$ - $T$  cooling curve and heating curve. The height of the quadrangle,  $\Delta\rho_\epsilon$ , as shown in Fig. 3a, suggests the amount of  $\epsilon$  martensite produced by the thermo-induced  $\gamma \rightarrow \epsilon$  martensitic transformation during cooling to 80 K. It can be seen in Fig. 3 that the  $\Delta\rho_\epsilon$  of Fe-27.7 Mn-4.1 Si alloy is greater than that of other alloys.

Fig. 4 shows the  $\rho$ - $T$  curves measured during thermal cycling between 80 K and 500 K. Cyclic  $\gamma \rightleftharpoons \epsilon$  transformation has an effect on the subsequent  $\gamma \rightarrow \epsilon$  martensitic transformation and the  $\epsilon \rightarrow \gamma$  reverse transformation. The  $M_S$ ,  $A_S$  and  $A_f$  temperature increase slightly over four thermal cycles. It was found that  $\epsilon$  martensite plate formation exhibits reproducibility [19].

### 3.3. Shape memory effect

The SME of Fe-27.7 Mn-4.1 Si, Fe-31.8 Mn-5.2 Si and Fe-32.0 Mn-6.1 Si alloys at various temperatures is shown in Table II. Bending temperature and microstructure have a strong effect on SME. For Fe-27.7 Mn-4.1 Si alloy,  $M_S$  is high and  $T_N$  is much lower than  $M_S$ ; there is a great deal of thermo-induced  $\epsilon$  martensite at room temperature, therefore, the austenite to be transformed to  $\epsilon$  martensite reduces so that the SME is smaller at room temperature. However, the SME becomes larger at higher temperature because the amount of thermo-induced  $\epsilon$  martensite formed before bending is less. The pre-existing thermo-induced  $\epsilon$  martensite is not favourable to SME. It can be seen that the SME of Fe-31.8 Mn-5.2 Si and Fe-32.0 Mn-6.1 Si are larger, and a good SME can be given over a wide temperature range. With  $(M_S - T_N)$  being smaller, the thermo-induced  $\gamma \rightarrow \epsilon$  martensitic transformation is suppressed, the pre-existing  $\epsilon$  martensite becomes smaller and smaller; the  $\epsilon$  martensite produced before bending is mostly stress induced, and the SME is good.

The extra volume expansion and antiferromagnetic ordering caused by Néel transition of the  $\gamma$  phase will reduce the free energy of the  $\gamma$  phase and increase the resistance to dislocation movement, so that the  $\gamma$  phase is stabilized against thermo-induced  $\gamma \rightarrow \epsilon$  martensitic transformation. However, the  $\gamma \rightarrow \epsilon$  martensitic transformation takes place when the alloys are affected by the force, although  $M_S$  is lower. When  $(M_S - T_N)$  is larger, the effect of Néel transition on the  $\gamma \rightarrow \epsilon$  transformation is weak. However, when  $(M_S - T_N)$  becomes smaller, the effect of the Néel transition on  $\gamma \rightarrow \epsilon$  transformation is strong, and the thermoinduced  $\gamma \rightarrow \epsilon$  martensitic transformation is suppressed. Therefore, there is an effect of the Néel transition on SME in which the thermoinduced  $\gamma \rightarrow \epsilon$  martensitic transformation is suppressed by antiferromagnetic order; in that way, the SME is improved.

## 4. Conclusions

1. Silicon reduces the Néel temperature and enhances the paramagnetic characteristic of  $\gamma$ -Fe-Mn alloy, which results in the anomalous increase of  $\rho$  below  $T_N$  being stronger. The anomalous  $\rho$  increases with increasing silicon content.

2. Silicon reduces the stabilization of austenite, which makes the stress-induced  $\gamma \rightarrow \epsilon$  martensitic transformation easier. The thermo-induced  $\gamma \rightarrow \epsilon$  martensitic transformation is suppressed when  $\gamma$  or  $\epsilon$  phases transfer from the paramagnetic to the antiferromagnetic state.

TABLE II SME at various temperatures for Fe-27.7 Mn-4.1 Si, Fe-31.8 Mn-5.2 Si and Fe-32.0 Mn-6.1 Si alloys

Code	SME (%)								
	79	257 K	273 K	288 K	297 K	310 K	323 K	340 K	360 K
1	-	-	-	35	35	-	-	61	43
2	-	-	-	78	77	78	80	61	-
3	75	74	86	85	84	79	72	53	41

3. In order to obtain a good SME, it is necessary to adjust the composition of the alloys so as to control the  $M_S$  and  $T_N$  to avoid thermo-induced  $\gamma \rightarrow \epsilon$  martensitic transformation.

4. Silicon increases the electrical resistivity and magnetic susceptibility of  $\gamma$ -Fe-Mn alloy.  $\epsilon$  phase obviously increases the electrical resistivity of Fe-Mn-Si alloys.

5. Cycling  $\gamma \rightleftharpoons \epsilon$  transformation elevates the  $M_S$ ,  $A_S$  and  $A_f$  temperatures of Fe-27.7 Mn-4.1 Si alloy.

### Acknowledgement

This work was supported by the National Science Foundation of China, under grant No. 59 171 021.

### References

1. E. GARTSTEIN and A. RABINKIN, *Acta Metall.* **27** (1979) 1053.
2. M. MURAKAMI, H. OTSUKA, H.G. SUZURI and S. MATSUDA, in "Proceedings of the International Conference on Martensitic Transformations", Nara, Japan, 1986, edited by The Japan Institute of Metals. (The Japan Institute of Metals, 1987) p. 985.
3. A. SATO, E. CHISHIMA, K. SOMA and T. MORI, *Acta Metall.* **30** (1982) 1177.
4. A. SATO, E. CHISHIMA, Y. YAMAJI and T. MORI, *ibid.* **32** (1984) 539.

5. A. SATO, Y. YAMAJI and T. MORI, *ibid.* **34** (1986) 87.
6. H. OTSUKA, H. YAMADA, T. MARUYAMA, H. TANAHASHI, S. MATSUDA and M. MURAKAMI, *ISIJ Int.* **30** (1990) 674.
7. H. OTSUKA, H. YAMADA, H. TANAHASHI and T. MARUYAMA, *Mater. Sci. Forum* **56-58** (1990) 655.
8. H. OTSUKA, M. MURAKAMI and S. MATSUDA, in "Proceedings of the MRS International Conference on Advanced Materials 'Shape Memory Materials'", Tokyo, Japan, 1988, vol. **9** (Materials Research Society, Pittsburgh; 1989) 451.
9. ZHANG YANSHENG, *Acta Metall. Sin.* **19** (1983) A260 (in Chinese).
10. *Idem, ibid.* **20** (1984) A313 (in Chinese).
11. *Idem, ibid.* **21** (1985) A295 (in Chinese).
12. *Idem, ibid.* **22** (1986) A470 (in Chinese).
13. *Idem, ibid.* **23** (1987) A306 (in Chinese).
14. *Idem, J. Phys. F. Met. Phys.* **18** (1988) L229.
15. *Idem, Mater. Sci. Prog.* **2** (1988) 56 (in Chinese).
16. ZHANG YANSHENG and ZENG HONGBIN, *J. Phys. Condensed Matter* **2** (1990) 2015.
17. QIN ZUOXIANG and ZHANG YANSHENG, *J. Phys. Condensed Matter*. (submitted).
18. H. OHNO and M. MEKATA, *J. Phys. Soc. Jpn.* **31** (1971) 102.
19. YU MANPING, QIN ZUOXIANG, ZHANG JIAJUN and ZHANG YANSHENG, *J. Dalian Railway Inst.* **14** (1) (1993) 54 (in Chinese).

Received 31 May  
and accepted 9 November 1995